

73. Intramolecular Dynamics of Tetranuclear Iridium Carbonyl Cluster Compounds

Part V¹⁾

Polysubstituted Derivatives of $[\text{Ir}_4(\text{CO})_{12}]$

by **Andrés Strawczynski, Chris Hall, Giacomo Bondietti, Renzo Ros²⁾, and Raymond Roulet***

Institut de Chimie Minérale et Analytique de l'Université, 3, place du Château, CH-1005 Lausanne

(4. II. 94)

The dynamic behaviour of twelve polysubstituted derivatives of $[\text{Ir}_4(\text{CO})_{12}]$ has been investigated in solution, using 2D-EXSY, and VT-³¹P- and ¹³C-NMR. $[\text{Ir}_4(\text{CO})_6(\mu_2\text{-CO})_3(\eta^4\text{-diarsine})\text{PPh}_3]$ and $[\text{Ir}_4(\text{CO})_6(\mu_2\text{-CO})_3(\eta^4\text{-norbornadiene})(\text{PMePh}_2)]$ exhibit two isomeric forms in solution, which interconvert through an intramolecular change of basal face. The related cluster $[\text{Ir}_4(\text{CO})_6(\mu_2\text{-CO})_3(\eta^4\text{-norbornadiene})\text{PPh}_3]$ exists as a single isomer in solution. It displays rotation of CO ligands about the apical Ir-atom, followed by two consecutive changes of basal face. The tetrasubstituted clusters with two chelating ligands $[\text{Ir}_4(\text{CO})_5(\mu_2\text{-CO})_3(\eta^4\text{-diolefin})_2]$ also exhibit rotation of apical CO's, the activation energy increases with greater steric hindrance of the radial ligands. A quantitative analysis of the ³¹P- and ¹³C-2D-EXSY spectra followed by simulation of the corresponding VT-NMR spectra of $[\text{Ir}_4(\text{CO})_5(\mu_2\text{-CO})_3(\mu_2\text{-L})_2]$ (L = bis(diphenylphosphino)methane and 1,3-bis(diphenylphosphino)propane) revealed a pairwise averaging of the P-atoms, caused by two parallel changes of basal face averaging all CO ligands. In addition, the restricted rotation of ligands about the apical Ir-atom was identified at higher temperatures. The remaining clusters are either rigid on the NMR time scale, or display CO-scrambling about a single Ir-atom.

Introduction. – The fluxional behaviour of monosubstituted $[\text{Ir}_4(\text{CO})_{11}\text{L}]$ clusters is now well documented (L = PEt₃ [2] [3], PMePh₂ [4], PH₂Ph, PPh₂ [5], PAr₃ [1], P(OR)₃ [6], H⁻ [7], Br⁻ [8], I⁻, NO₂⁻, SCN⁻ [1], SO₂ [9], *t*-BuNC, ArNC [10] [11], $\overline{\text{COCH}_2\text{CH}_2\text{O}}$ [12]). The pathways for CO scrambling in disubstituted $[\text{Ir}_4(\text{CO})_{10}\text{L}_2]$ clusters with monodentate L ligands are more complex, and only the scrambling processes of lowest activation energy in $[\text{Ir}_4(\text{CO})_{10}(\text{PMePh}_2)_2]$ have been identified to date [1]. The fluxional behaviour of two disubstituted complexes with one chelating ligand, $[\text{Ir}_4(\text{CO})_{10}(\text{cycloocta-1,5-diene})]$ and $[\text{Ir}_4(\text{CO})_{10}(\text{diarsine})]$, and of four disubstituted complexes with one edge-bridging bidentate ligand, $[\text{Ir}_4(\text{CO})_{10}(\mu_2\text{-L})]$ (L = bis(diphenylphosphino)methane and 1,3-bis(diphenylphosphino)propane, bis(diphenylarsino)methane, CH₃SCH₂SCH₃) have been examined in preceding articles of this series [13] [1].

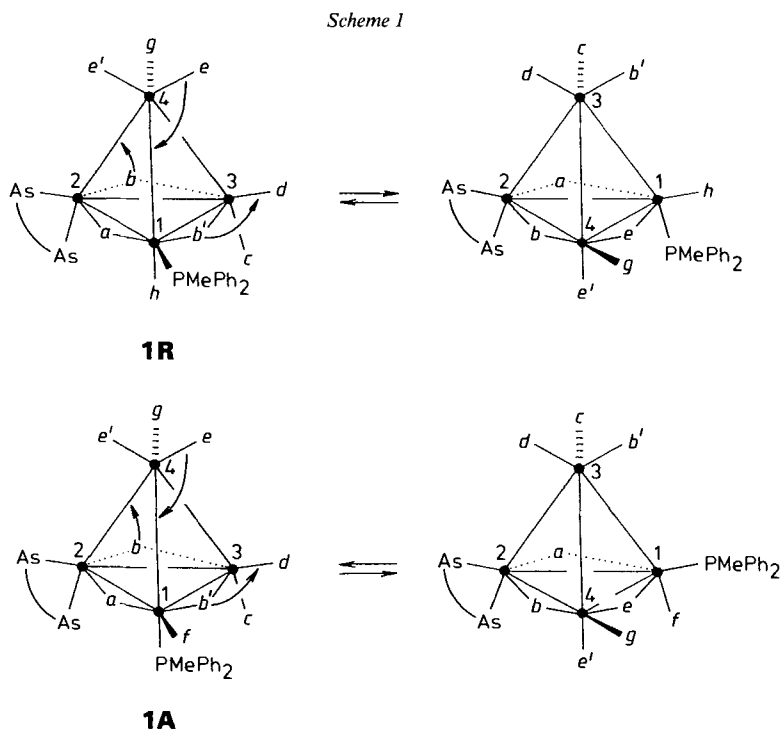
Polysubstituted derivatives of $[\text{Ir}_4(\text{CO})_{12}]$ were thought to be inert on the NMR time scale [14]. However, the trisubstituted cluster $[\text{Ir}_4(\text{CO})_6(\mu_2\text{-CO})_3(\mu_3\text{-1,3,5-trithiane})]$ is indeed fluxional [15], a variable-pressure NMR study afforded the first detailed picture of the merry-go-round process [16]. We now report on the intramolecular dynamics of two more trisubstituted clusters with a face-capping ligand and of ten polysubstituted derivatives of $[\text{Ir}_4(\text{CO})_{12}]$ whose ground-state geometries preclude the merry-go-round process.

¹⁾ Part IV: [1].

²⁾ Permanent address: Istituto di Chimica Industriale dell'Università, Via Marzolo 9, I-35131 Padova.

Trisubstituted Complexes. – 1. *With One Chelating Bidentate Ligand.* The reaction of $[\text{Ir}_4(\text{CO})_{10}(\text{diarsine})]$ with 1 mol-equiv. of PPh_3 in THF at 0° in the presence of Me_3NO followed by chromatography afforded $[\text{Ir}_4(\text{CO})_6(\mu_2\text{-CO})_3(\eta^4\text{-diarsine})\text{PPh}_3]$ (**1**) in 66% yields. Its IR spectrum in cyclohexane shows two bands below 1900 cm^{-1} indicating the presence of bridging CO's. The ^{31}P -NMR spectrum of **1** in CD_2Cl_2 at 183 K presents two resonances at 25.6 and -3.0 ppm relative to external H_3PO_4 85%. Their coordination chemical shift ($\Delta\delta = 30.1$ and 1.5 ppm, respectively) are characteristic of P-atoms in radial and axial positions. Therefore, two isomers are present in solution, one with the PPh_3 ligand located on one basal Ir-atom in a radial (**1R**, Scheme 1) or axial position (**1A**). The equilibrium constant, $K = [\mathbf{1R}]/[\mathbf{1A}]$, was 1.43 at 183 K. The ratio of the two isomers changes reversibly upon varying the temperature, the formation of **1A** being endothermic. A two site P-exchange is observed above 183 K and the equilibrium constants $K = f(T)$ were calculated in the slow-exchange domain (183–238 K) from the relative intensities of the two signals. The thermodynamic parameters of isomerisation **1A** \rightarrow **1R** were calculated by linear regression of the function $\ln K = \Delta S^\circ/R - (\Delta H^\circ/RT)$ giving $\Delta H^\circ = -3.3 \pm 0.4\text{ kJ mol}^{-1}$ and $\Delta S^\circ = -15 \pm 4\text{ J mol}^{-1}\text{ K}^{-1}$ at 298 K. The variable-temperature ^{31}P -NMR spectra were then simulated using the following exchange matrix: $(P_R, P_R) = -k_1$, $(P_A, P_A) = -Kk_1$, $(P_R, P_A) = k_1$, and $(P_A, P_R) = Kk_1$, where k_1 = rate constant of process **1A** \rightarrow **1R**. A ^{13}C -NMR study was clearly needed to identify the mechanism of this isomerisation.

In the ^{13}C -NMR spectrum of a ^{13}C -enriched sample of **1** (ca. 30% ^{13}CO) in CD_2Cl_2 , all exchanges are blocked at ca. 190 K, and two sets of nine CO resonances are observed (see *Exper. Part*). Six resonances appear in the region of $\mu_2\text{-CO}$'s, indicating that both isomers



have a basal face with three edge-bridging CO's and C_1 symmetry. Three signals are observed in the region of radial CO's (d_R, f_A , and d_A in *Scheme 1*) confirming the relative positions of the PPh_3 ligand in the two isomers. Upon raising the temperature to 273 K, two pairs of signals due to bridging CO's (a_A, a_R and b_A, b_R) do not exchange with those of terminal CO's. An intermediate or transition state with all terminal CO's may, therefore, be excluded. A 2D-EXSY spectrum of **1** in CD_2Cl_2 at 203 K showed the following exchanges (each involving one signal of **1A** and one of **1R**): $a_R \leftrightarrow a_A$, $b_A \leftrightarrow b_R$, $b'_A \leftrightarrow e_R$, $b'_R \leftrightarrow e_A$, $d_R \leftrightarrow g_A$, $f_A \leftrightarrow h_R$, $d_A \leftrightarrow g_R$. The signals due to CO's c and e' are also exchanging pairwise. Therefore, the CO-scrambling process with lowest activation energy, responsible for the interconversion $\mathbf{1A} \rightleftharpoons \mathbf{1R}$ is a synchronous change of basal face (*Scheme 1*). This process is similar to that previously observed for $[Ir_4(CO)_{10}(\text{diarsine})]$ [13]. Too many signals were present for a complete line-shape analysis of the variable-temperature ^{13}C -NMR spectra. However, the two site exchange $a_A \leftrightarrow a_R$ was simulated using the same exchange matrix as that used for the ^{31}P -NMR spectra. All ^{13}C - and ^{31}P -NMR data were then used in an Eyring regression of $\ln(k_i/T)$ vs. $1/T$ (*Fig. 1*). This gave a free enthalpy of

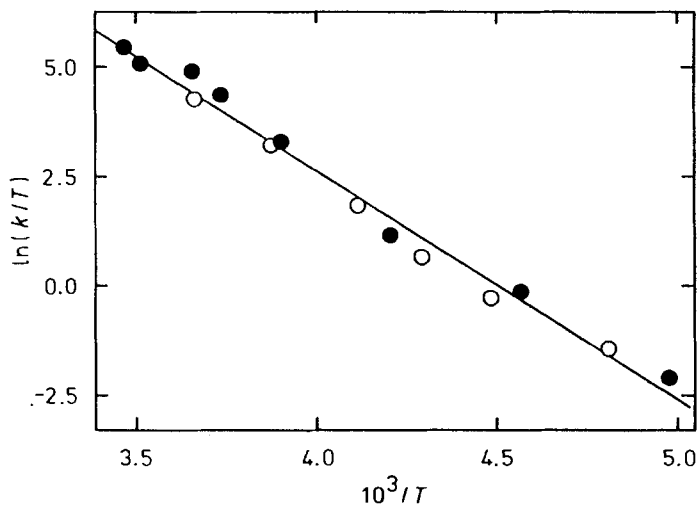
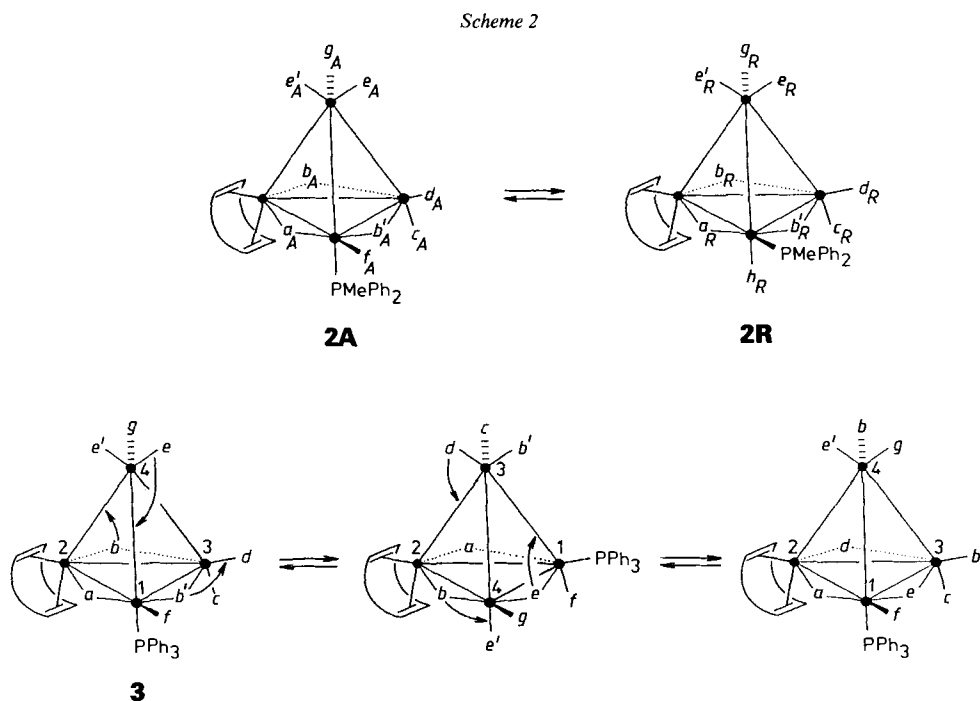


Fig. 1. Eyring regression of both ^{31}P (●) and ^{13}C -NMR (○) data for **1**

activation of $44.1 \pm 0.8 \text{ kJ mol}^{-1}$ (at 298 K) for the isomerisation $\mathbf{1A} \rightleftharpoons \mathbf{1R}$ (a value of $43.9 \pm 1 \text{ kJ mol}^{-1}$ was obtained from the ^{31}P -NMR data alone). Above 273 K, the coalesced signals due to (a_R, a_A) and (b_A, b_R) start to broaden due to exchanges with signals of apical CO's, consistent with a second change of basal face. This process is assumed to pass through an unbridged intermediate, but could not be simulated since the assignment of CO's c and e' is ambiguous (a 2D-COSY spectrum only proves the pseudo-*trans*-relationship of the corresponding signals).

The trisubstituted cluster $[Ir_4(CO)_6(\mu_2-CO)_3(\eta^4\text{-nbd})L]$ (nbd = norbornadiene; L = PMe_2Ph , $PMePh_2$ (**2**), PPh_3 (**3**), $AsPh_3$) are known, and the crystal structures of the radial isomer with L = PMe_2Ph and of the axial isomer with L = PPh_3 have been already

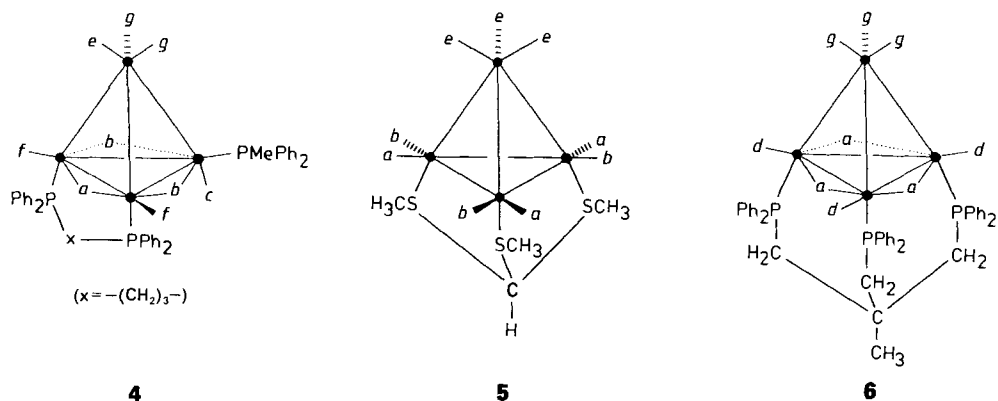
reported [17]. The ^{31}P -NMR spectrum of **2** in CD_2Cl_2 at 193 K consists of two resonances at $\delta -37.0$ and -8.3 ppm ($\Delta\delta = -8.7$ and $+20$ ppm, respectively). As observed for **1**, two isomers are present in solution with the PMePh_2 ligand either in a radial (**2R**) or axial (**2A**, Scheme 2). The calculated equilibrium constant $K = [\mathbf{2A}]/[\mathbf{2R}]$ was 1.8 ± 0.1 at 193 K. The ^{13}C -NMR and 2D-COSY spectra of a ^{13}C -enriched sample of **2** in CD_2Cl_2 confirmed the proposed ground-state geometries of both isomers (see *Exper. Part*). On raising the temperature close to the boiling point of the solvent, exchanges involving one signal of **2R** and one of **2A** take place as observed in **1**. These could not be simulated, due to sample decomposition above 40° .



The related cluster **3** is present as a single, observable isomer in solution whose ground-state geometry was proposed to be the same as in the solid state, on the basis of its coordination chemical shift $\Delta\delta(\text{P})$ (Scheme 2) [17]. The ^{13}C -NMR spectrum of a ^{13}C -enriched sample of **3** in $\text{C}_2\text{D}_2\text{Cl}_4$ at 240 K consists of eight CO signals which were assigned by comparison with those of **2A** (see *Exper. Part*). The presence of two signals in the region of radial CO's (one of which displays a geminal C,P coupling) was in agreement with an axial position of the PPh_3 ligand. Upon raising the temperature, only the signals of CO's e , e' , and g broaden, and coalesce at *ca.* 310 K. Therefore, the CO-scrambling process with lowest activation energy is the rotation of three CO's about the apical Ir-atom. Above 310 K, a second process leads to broadening of the resonances of CO's b , d , and either a or b' which have the same δ 's. The resonances due to c , f , and either a or b' remain

sharp. A full simulation of this second process was thwarted by sample decomposition above 340 K. As resonances due to a radial isomer were not observed, a mechanism to account for the broadening of the resonances must lead to restoration of the ground-state geometry. There are two equivalent mechanisms which satisfy all these conditions, both of which involve two consecutive changes of basal face (Ir(1)–Ir(2)–Ir(3) and Ir(1)–Ir(2)–Ir(4)). For clarity, only one of these is shown in *Scheme 2*. The following exchanges are expected: $a \leftrightarrow a$, $b \leftrightarrow (g \text{ or } d)$, $b' \leftrightarrow (d \text{ or } e)$, $c \leftrightarrow c$, $d \leftrightarrow (b \text{ or } b')$, $e \leftrightarrow (b' \text{ or } g)$, $e' \leftrightarrow e'$, $f \leftrightarrow f$, and $g \leftrightarrow (e \text{ or } b)$. This mechanism is consistent with the observation that c , f , and one of the bridging CO's do not exchange (at these temperatures, the three apical CO's present only one broad signal and further exchanges involving these cannot be resolved). The proposed, consecutive changes of basal face are comparable to those observed in the interconversion $1A \rightleftharpoons 1R$.

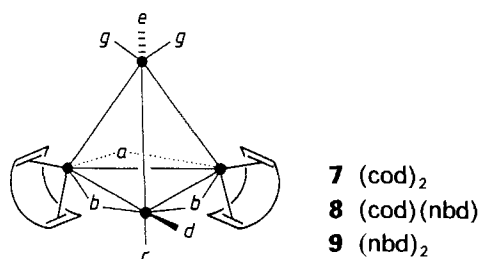
2. *With One Edge-Bridging Bidentate Ligand*. The reaction of $[\text{Ir}_4(\text{CO})_{10}(\mu_2\text{-dppp})]$ (dppp = 1,3-bis(diphenylphosphino)propane) with PMePh_2 in toluene followed by chromatography gave $[\text{Ir}_4(\text{CO})_6(\mu_2\text{-CO})_3(\mu_2\text{-dppp})(\text{PMePh}_2)]$ (**4**, 58%), with the corresponding tetrasubstituted complex as a minor product. Cluster **4** has three bridging CO's defining the basal face, the dppp ligand in diaxial position and PMePh_2 in a radial position, as shown by its IR, ^{31}P - and ^{13}C -NMR spectra (see *Exper. Part*). It is not fluxional in solution up to the boiling point of CD_2Cl_2 in a sealed tube.



3. *With One Face-Capping, Tridentate Ligand*. The cluster $[\text{Ir}_4(\text{CO})_9\{\text{HC}(\text{SCH}_3)_3\}]$ (**5**) was obtained from the reaction of $[\text{Ir}_4(\text{CO})_{11}\text{Br}]^-$ with 1 mol-equiv. of tris(methylthio)methane in the presence of AgBF_4 . In contrast to $[\text{Ir}_4(\text{CO})_6(\mu_2\text{-CO})_3(\mu_3\text{-}1,3,5\text{-trithiane})]$ [**15**] [16], it has a ground-state geometry with all terminal CO's. The ^{13}C -NMR spectrum of a ^{13}C -enriched sample of **5** in CD_2Cl_2 at 190 K shows three signals of equal relative intensities at δ 166.2, 166.1 (a and b), and 156.4 ppm (e). The magnetic nonequivalence of the basal CO's is a consequence of the relative positions of the Me groups which cannot reside on the planes passing through one S, two Ir-atoms and the mid-point of one basal Ir–Ir bond. Upon raising the temperature, the two signals with highest δ 's coalesce. This could be due to the merry-go-round of the six basal CO's.

Similar dynamic behaviour has already been reported for $[\text{Ir}_4(\text{CO})_9\{\text{HC}(\text{PPh}_2)_3\}]$, whose crystal structure is known [18]. We were able to simulate its variable-temperature ^{13}C -NMR spectra with an exchange matrix corresponding to the merry-go-round ($\Delta G^\ddagger = 43.3 \pm 0.4 \text{ kJ mol}^{-1}$ at 298 K; see *Exper. Part*). However, the coalescence of the signals of *a* and *b* could equally be due to averaging of the orientations of the Ph groups of the tripod ligand with respect to the three planes of symmetry. The multiplicity of the signal of CO's *e* corresponds to an $AA'A''XX'X''$ spin system at 183 K, but is a *quadruplet* ($^3J(\text{C,P}) = 13 \text{ Hz}$) at 300 K. The equal coupling of three equivalent CO's to the three P-atoms of the tripod ligand requires that rotation of apical CO's is also taking place in this complex. The ^{13}C -NMR spectrum of the related cluster $[\text{Ir}_4(\text{CO})_6(\mu_2\text{-CO})_3(\mu_3\text{-triphos})]$ (triphos = 1,3-bis(diphenylphosphino)-2-[(diphenylphosphino)methyl]-2-methylpropane, **6**) corresponds to a ground-state geometry of C_{3v} symmetry with three edge-bridging CO's (see *Exper. Part*). No merry-go-round of basal CO's could be detected in this complex up to 313 K in CD_2Cl_2 .

Tetrasubstituted Complexes. – 1. *With Two Chelating Bidentate Ligands.* The cluster $[\text{Ir}_4(\text{CO})_5(\mu_2\text{-CO})_3(\eta^4\text{-cod})_2]$ (**7**) (cod = cycloocta-1,5-diene) has been prepared by *Shapley* and coworkers [14] from $[\text{Ir}_4(\text{CO})_{12}]$. It may also be obtained under milder conditions from $[\text{Ir}_4(\text{CO})_{11}\text{Br}]^-$, or by selective oxidation of $[\text{Ir}_4(\text{CO})_{10}(\eta^4\text{-cod})]$ by Me_3NO in the presence of 1 mol-equiv. of cod [19]. We have now prepared $[\text{Ir}_4(\text{CO})_5(\mu_2\text{-CO})_3(\eta^4\text{-cod})(\eta^4\text{-nbd})]$ (**8**), and $[\text{Ir}_4(\text{CO})_5(\mu_2\text{-CO})_3(\eta^4\text{-nbd})_2]$ (**9**) by similar routes. The IR and NMR data of these compounds suggest a ground-state geometry with three edge-bridging CO's and C_s (**7**, **9**) or C_1 symmetry (**8**; see *Exper. Part*). They all exhibit the same fluxional behaviour in solution. The exchange matrices were deduced from the corresponding 2D-EXSY spectra (example shown for **9** in *Fig. 2*). The only CO-scrambling process is the rotation of apical CO's. Simulation of the variable-temperature ^{13}C -NMR spectra in CD_2Cl_2 followed by *Eyring* regressions of $\ln(k/T)$ vs. $1/T$ gave the free enthalpies of activation of



62.2 ± 0.3 , 53.2 ± 0.4 , and $46.7 \pm 0.6 \text{ kJ mol}^{-1}$ at 298 K for **7**, **8**, and **9**, respectively. The same sequence of decreasing ΔG^\ddagger 's was observed for the corresponding derivatives of $[\text{Ir}_3\text{Rh}(\text{CO})_{12}]$ and $[\text{Ir}_2\text{Rh}_2(\text{CO})_{12}]$ [20], and is probably due to a decrease of steric hindrance by the C=C bonds in radial positions on going from a 1,5- to a more strained 1,4-diene.

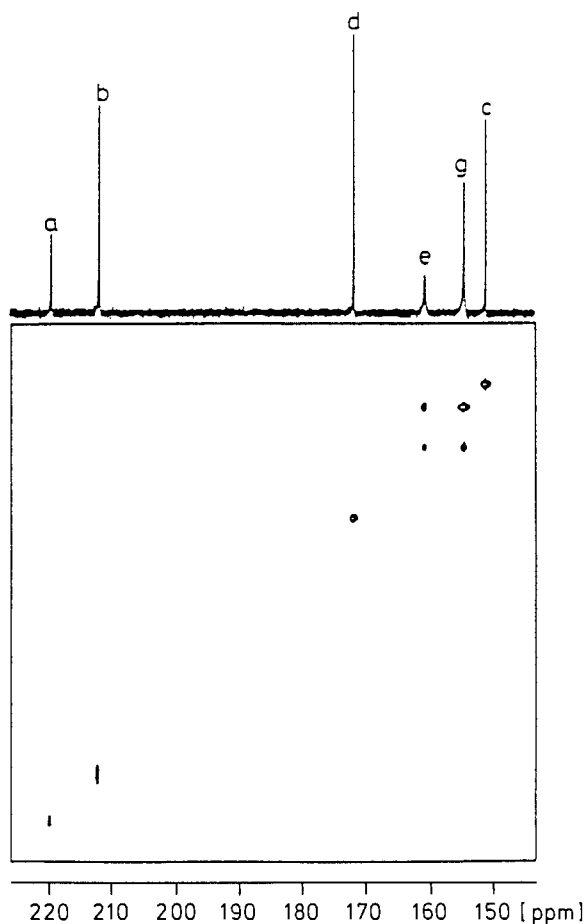
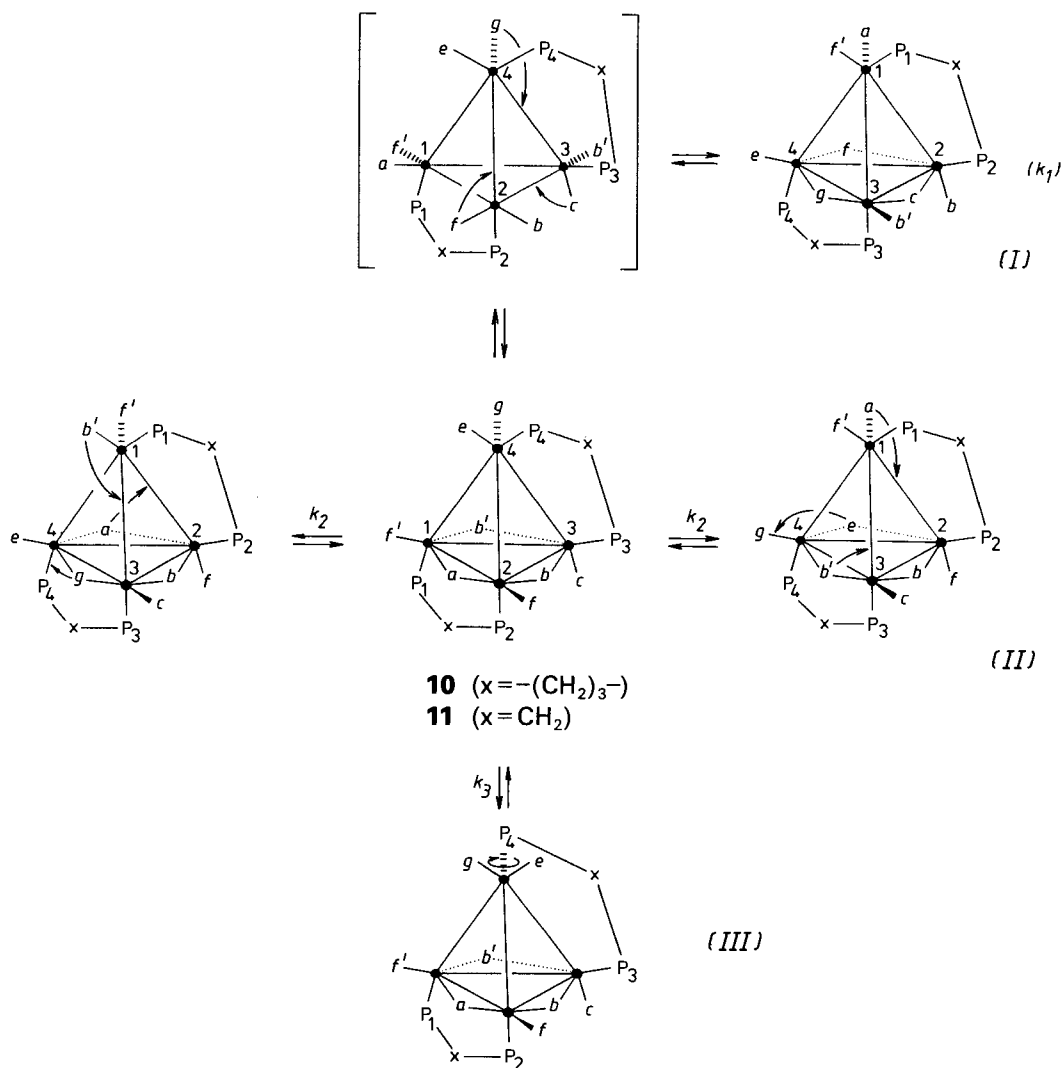


Fig. 2. ^{13}C -EXSY Spectrum of **9** in CD_2Cl_2 at 213 K (mixing time: 100 ms)

2. *With Two Edge-Bridging, Bidentate Ligands.* The ^{13}C -NMR spectrum of a ^{13}C -enriched sample of $[\text{Ir}_4(\text{CO})_5(\mu_2\text{-CO})_3(\mu_2\text{-dppp})_2]$ (**10**) in CD_2Cl_2 at 290 K has three resonances in the region of bridging CO's, two in the region of radial CO's, and one in the region of apical CO's displaying a pseudo-*trans*-C,P-coupling. Its ^{31}P -NMR spectrum exhibits four resonances, one of these with a $\Delta\delta$ typical of a P-atom in radial position (P_3) and two with $\Delta\delta$'s corresponding to axial positions (P_1 , P_2 , see *Exper. Part*). P_1 can be distinguished from P_2 by its large pseudo-*trans*-coupling with P_4 . The data are in agreement with a ground-state geometry in which one dppp ligand occupies two axial positions with respect to the basal plane, and the other one bridges an apical and the third basal Ir-atom (*Scheme 3*). The ^{13}C - and ^{31}P -NMR spectra of the related cluster $[\text{Ir}_4(\text{CO})_5(\mu_2\text{-CO})_3(\mu_2\text{-dppm})_2]$ (**11**, dppm = bis(diphenylphosphino)methane) at 185 K are quite similar to those of **10**, and the proposed ground-state geometry is the same as that found in the solid state [21].

Scheme 3



Cluster **10** is fluxional on the NMR time scale above 330 K in $\text{C}_2\text{D}_2\text{Cl}_4$. However, it slowly decomposes above 360 K, preventing a detailed study by variable-temperature NMR and conventional line-shape analysis. In principle, the dynamic connectivities may be obtained directly from 2D-EXSY spectra, although this can be complicated by the presence of second-order peaks. A quantitative evaluation of a 2D-EXSY spectrum can distinguish between first and second-order cross-peaks [22] [23] [7], thus providing the correct exchange matrix and accurate rate constants.

The ^{31}P -2D-EXSY spectrum of **10** in $\text{C}_2\text{D}_2\text{Cl}_4$ at 330 K with a mixing time of 30 ms shows exchange cross-peaks between P_1 and P_4 , and P_2 and P_3 (Fig. 3). The quantitative

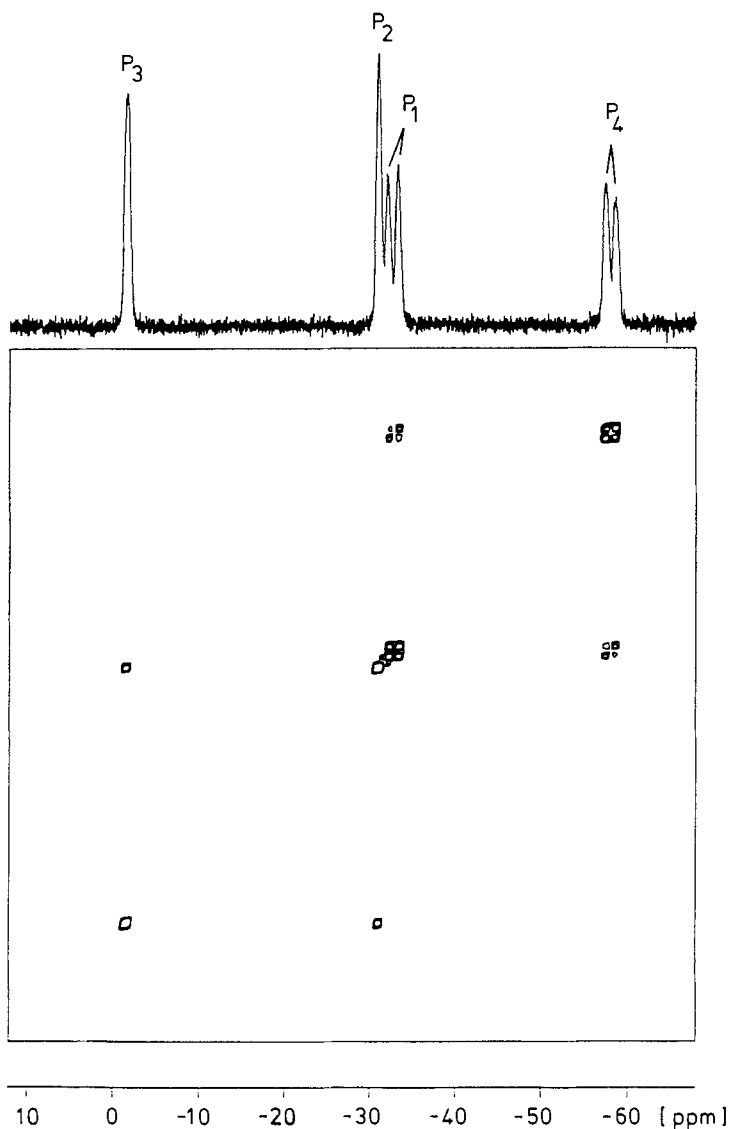


Fig. 3. ^{31}P -EXSY Spectrum of **10** in $\text{C}_2\text{D}_2\text{Cl}_4$ at 330 K (mixing time: 30 ms)

treatment of this spectrum using the D2DNMR program [22] gave rate constants for the $\text{P}_1 \leftrightarrow \text{P}_4$ and $\text{P}_2 \leftrightarrow \text{P}_3$ exchanges of 10.7 ± 0.4 and $10.2 \pm 0.5 \text{ s}^{-1}$, respectively. These are the same within experimental error (mean value $10.5 \pm 0.5 \text{ s}^{-1}$). The two pairs of P-atoms are symmetrically related by rotation about a C_2 axis passing through the mid-points of the Ir(1)–Ir(4) and Ir(2)–Ir(3) bonds of the Ir_4P_4 fragment. The same symmetry operation relates the two faces Ir(1)–Ir(2)–Ir(3) and Ir(3)–Ir(4)–Ir(2). Therefore, CO-scrambling processes involving this change of basal face should lead to the observed P-atom ex-

change (*Scheme 3*). This hypothesis was tested by a quantitative evaluation of a ^{13}C -2D-EXSY spectrum of **10** also at 330 K with a mixing time of 80 ms (*Fig. 4*). Four intense cross-peaks are observed between (1,7), (2,5), (3,4), and (4,6), the resonances being labelled in order of decreasing δ 's. Less intense cross-peaks are also observed, of which only (3,7) was shown to be second-order. This shows that two processes are occurring

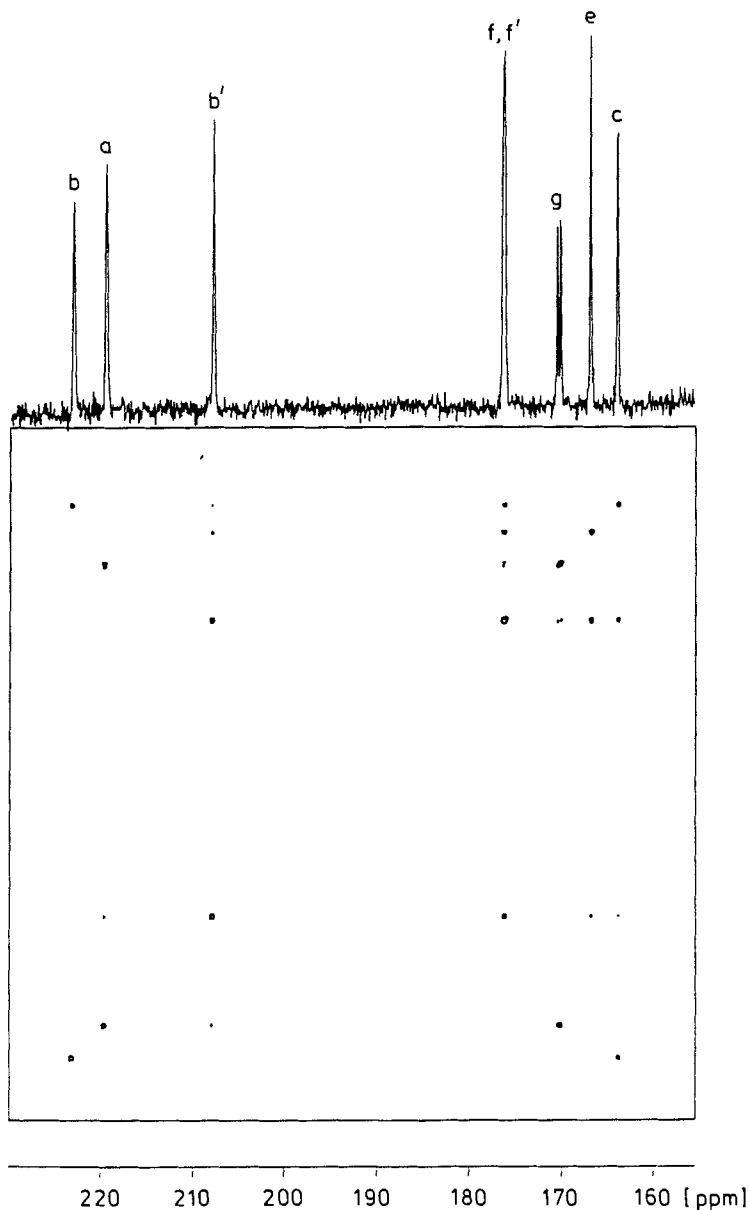


Fig. 4. ^{13}C -EXSY Spectrum of **10** in $\text{C}_2\text{D}_2\text{Cl}_4$ at 330 K (mixing time: 80 ms)

at this temperature with rate constants k_1 and k_2 . The following exchange matrix elements were obtained: $(1,7) = 7.3(9) = k_1$; $(2,3) = 1.8(5) = k_2$; $(2,5) = 9.7(14) = k_1 + k_2$; $(3,4) = 7.2(8) = k_1$; $(3,6) = 1.2(5) = k_2$; $(4,5) = 1.0(1) = k_2/2$; $(4,6) = 4.5(2) = (k_1 + k_2)/2$; $(4,7) = 1.9(2) = k_2$. For each element, the numerical entry results from the analysis of the 2D-EXSY spectrum, with the σ value in parentheses. Only those values for which statistically significant (2σ), positive values were obtained in both diagonally equivalent positions are shown. The second entry shows the algebraic form in terms of the rate constants k_1 and k_2 , assuming that k_1 is the rate constant of the change of basal face passing through an unbridged intermediate (*Scheme 3, mechanism I*) and k_2 that of the synchronous change of basal face (*mechanism II*). All the cross-peaks expected from these mechanisms are observed: $(b,c) = (b',f) = k_1$; $(a,g) = 2(f',e) = k_1 + k_2$; $(a,b') = (b',e) = 2(f',g) = (f,c) = k_2$. The mean values of k_1 and k_2 were found to be 7.3 ± 1.2 and $1.8 \pm 0.4 \text{ s}^{-1}$, respectively. Since both changes of basal face (*I* and *II*) lead to the pairwise exchanges $P_1 \leftrightarrow P_4$ and $P_2 \leftrightarrow P_3$, the rate constant obtained from the ^{31}P -EXSY analysis ($10.5 \pm 0.5 \text{ s}^{-1}$) should correspond to the sum $(k_1 + 2k_2) = 10.9 \pm 0.6 \text{ s}^{-1}$ (there are two equivalent mechanisms for the synchronous change of basal face (k_2)). The results obtained from the ^{13}C - and ^{31}P -NMR data are in excellent agreement.

The variable-temperature ^{31}P -NMR spectra of **11** up to 268 K show the same pairwise exchanges as observed for **10** and were successfully simulated using the following exchange matrix elements: $(P_n, P_n) = -k$ ($n = 1-4$); $(P_1, P_4) = (P_4, P_1) = (P_2, P_3) = (P_3, P_2) = k$, and taking into account the spin-state multiplicities (*Fig. 5, a*). At ca. 270 K, two resonances are present with δ 's equal to $(\delta(P_1) + \delta(P_4))/2$ and $(\delta(P_2) + \delta(P_3))/2$, respectively.

The variable-temperature ^{13}C -NMR spectra of a ^{13}C -enriched sample of **11** (*Fig. 5, b*) were successfully simulated using an 8×8 exchange matrix based on that invoked in the analysis of the ^{13}C -2D-EXSY spectrum of **10** (in this case CO's f and f' exhibit distinct resonances): $(1,1) = -k_1$; $(n,n) = -k_1 - k_2$ ($n = 2$ to 8); $(1,7) = (7,1) = (2,8) = (3,5) = (5,3) = (4,6) = k_1$; $(2,3) = (3,6) = (4,8) = (5,7) = (7,5) = k_2$; $(6,4) = (8,2) = k_1 + k_2$. The two mechanisms (*I* and *II, Scheme 3*) result in complete averaging of all CO signals, but averaging of the P-nuclei in pairs. Thus, between 270 and 300 K one observes a single resonance in the ^{13}C -NMR, but two in the ^{31}P -NMR spectra.

Above ca. 268 K, a new process results in the coalescence of the two remaining ^{31}P -resonances. This was observed in $\text{C}_2\text{D}_2\text{Cl}_4$, which has a higher boiling point than CD_2Cl_2 , and was successfully simulated using a two site exchange matrix (*Fig. 5, a*, rate constant k_3). Several mechanisms may be envisaged, of which the simplest is a restricted rotation at Ir(4) which would average P_1 and P_2 (*Scheme 3, III*). Eyring regressions of the ^{31}P - and ^{13}C -NMR data are shown in *Fig. 6*. The change of basal face through an unbridged intermediate (k_1) is a considerably lower-energy process than the synchronous basal face change (k_2). Therefore, the exchange of P-atoms is dominated by k_1 with only a small contribution from k_2 .

The ^{13}C -NMR data gave the following free enthalpies of activation at 298 K: $\Delta G_1^\ddagger = 38.1 \pm 0.5$ (k_1) and $\Delta G_{II}^\ddagger = 47.1 \pm 0.5 \text{ kJ mol}^{-1}$ (k_2). The values calculated from the ^{31}P -NMR data were: $\Delta G_1^\ddagger = 38.4 \pm 1.2$ and $\Delta G_{III}^\ddagger = 62.3 \pm 0.6 \text{ kJ mol}^{-1}$ (k_3), showing a very good agreement between both values of ΔG_1^\ddagger .

From a partial simulation ($320 < T < 370 \text{ K}$) of the ^{13}C -NMR data of **10**, the corresponding parameters were: $\Delta G_1^\ddagger = 76 \pm 2$ (k_1), and $\Delta G_{II}^\ddagger = 78 \pm 3 \text{ kJ mol}^{-1}$ (k_2). Similar treatment of the ^{31}P -NMR data gave $\Delta G_1^\ddagger = 75 \pm 2 \text{ kJ mol}^{-1}$. Cluster **11**, containing the

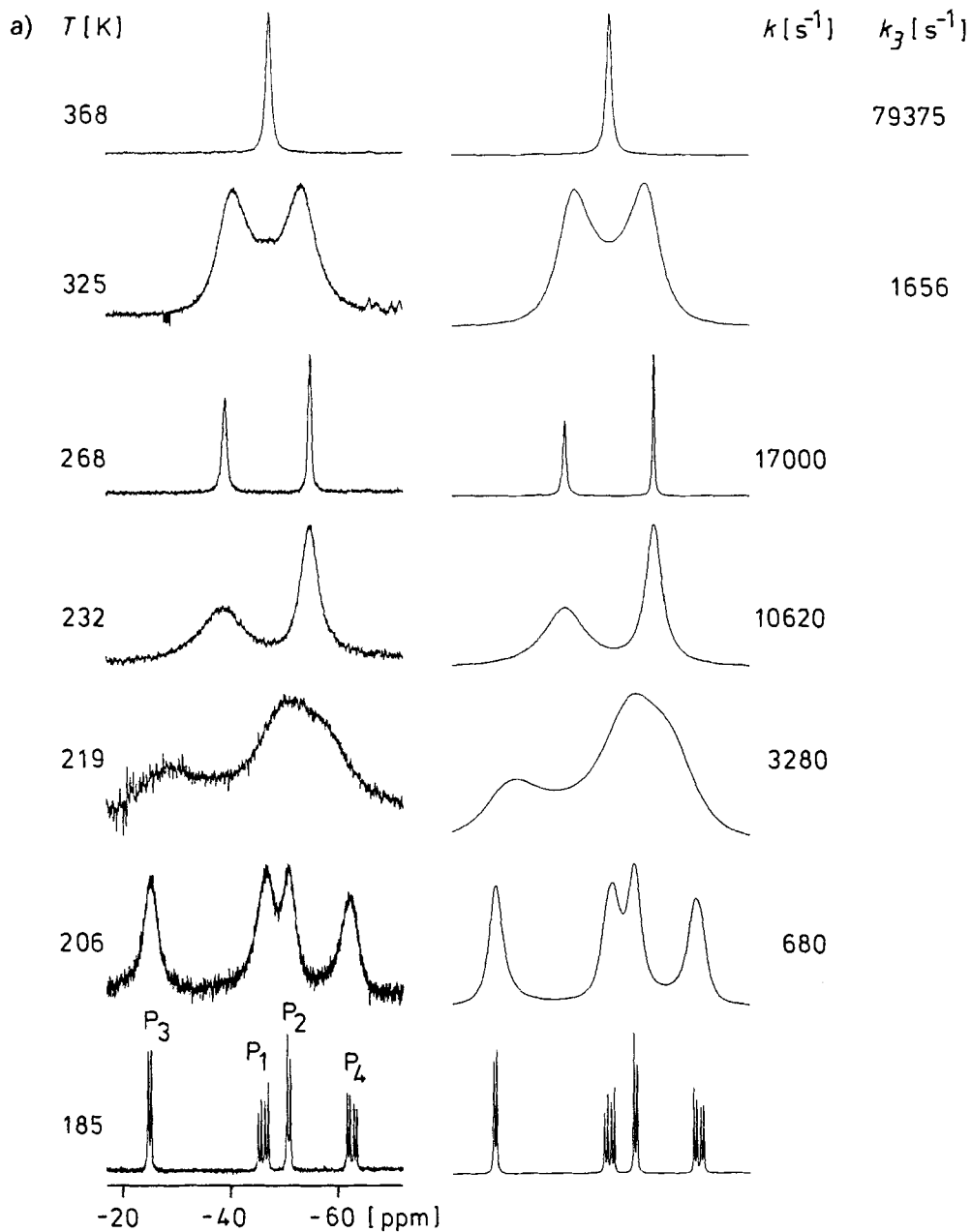


Fig. 5. Variable-temperature ^{31}P -NMR (a) and ^{13}C -NMR (b) spectra of **11** in CD_2Cl_2 (in $C_2D_2Cl_4$ for (a) above 270 K)

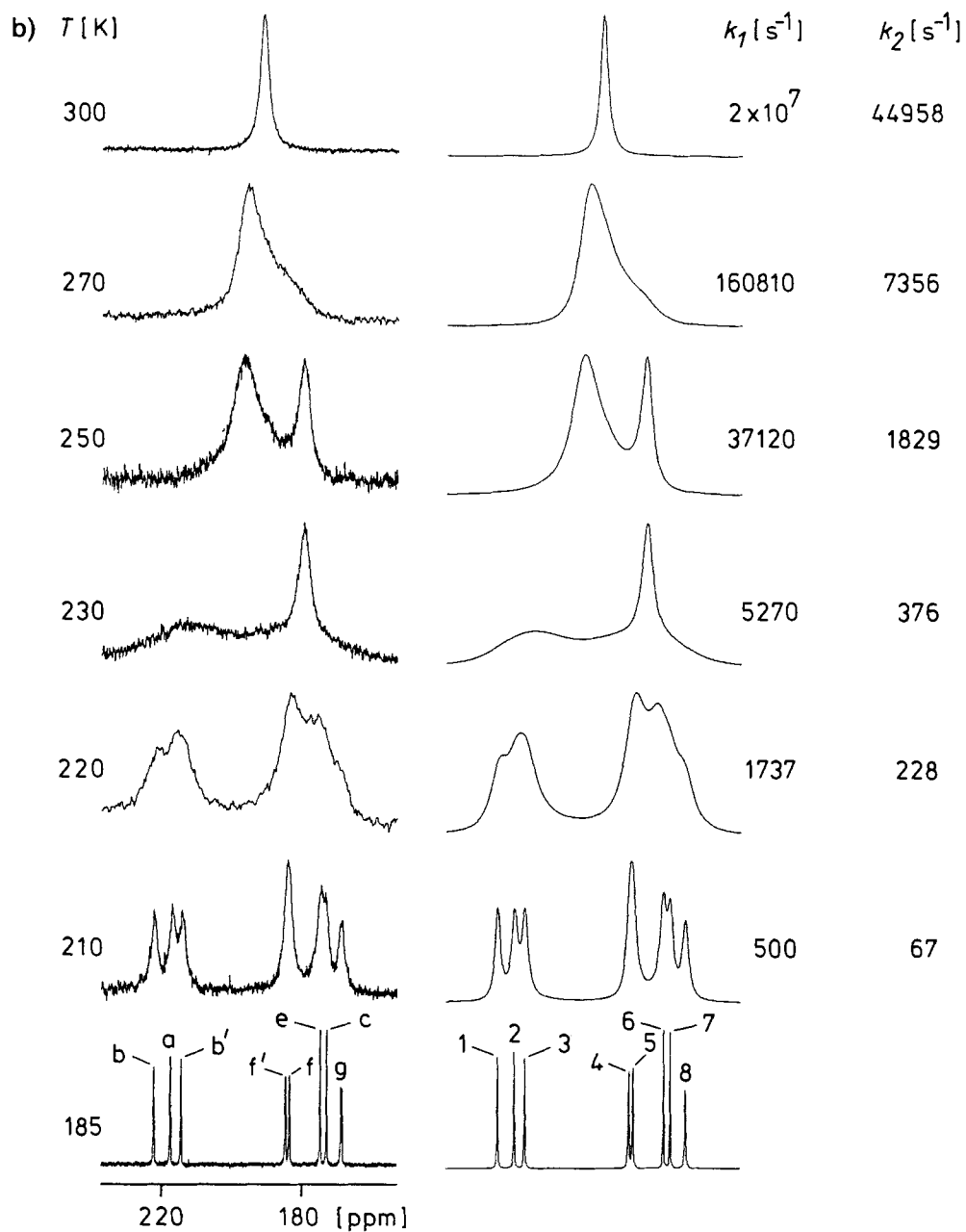


Fig. 5 (cont.)

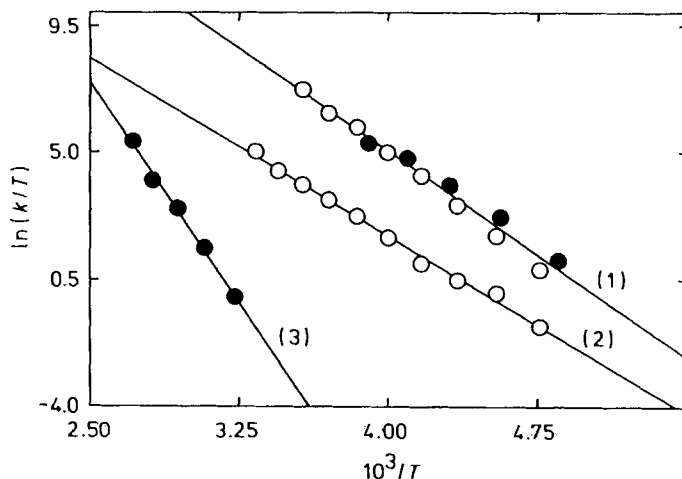
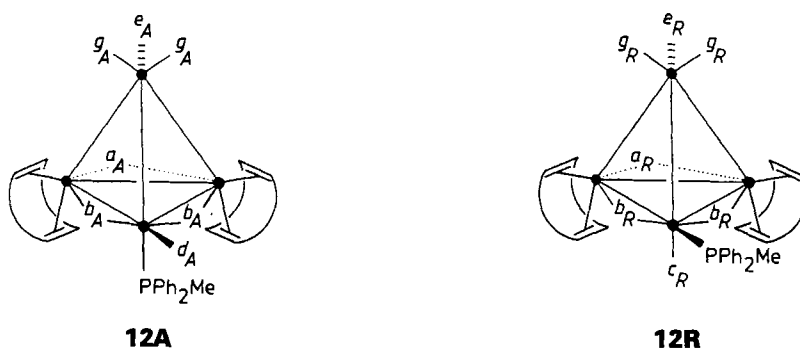


Fig. 6. Eyring regression of both ^{31}P (●) and ^{13}C -NMR (○) data for **11** (rate constants k_1 (1) and k_2 (2) in CD_2Cl_2 , rate constants k_3 (3) in $\text{C}_2\text{D}_2\text{Cl}_4$)

bidentate ligand with smallest bite angle, is significantly more fluxional than **10**. The same trend has already been observed between $[\text{Ir}_4(\text{CO})_{10}(\mu_2\text{-dppm})]$ and $[\text{Ir}_4(\text{CO})_{10}(\mu_2\text{-dppp})]$ [1]. We are currently undertaking an X-ray analysis of **10** for comparison with the known structure of **11** [21], with the aim of identifying differences in ground-state geometry which could lead to such marked differences in dynamic behaviour.

Pentastituted Complexes. – The ^{31}P -NMR spectrum of $[\text{Ir}_4(\text{CO})_4(\mu_2\text{-CO})_3(\eta^4\text{-nbd})_2(\text{PMePh}_2)]$ [17] in CD_2Cl_2 at 183 K presents two resonances at $\delta -41.5$ and -9.3 ($\Delta\delta = -13.2$ and $+18.5$ ppm, respectively). Therefore, two isomers are present in solution with the PMePh_2 ligand either in axial (**12A**, major species) or radial position (**12R**) with



respect to the basal plane. There is no interconversion between the isomers upon heating the solution to 60° in a sealed tube. The ^{13}C -NMR spectrum of a ^{13}C -enriched sample of **12** in CD_2Cl_2 at 183 K presents two pairs of signals in the region of bridging CO's, each with relative intensities 1:2. Only one signal (d_A) is present in the region of radial CO's (see

Exper. Part), in agreement with the proposed ground-state geometries. A 2D-EXSY spectrum taken at 228 K (mixing time: 100 ms) showed the dynamic connectivities $e_A \leftrightarrow g_A$ and $e_R \leftrightarrow g_R$. Therefore, CO scrambling takes place independently in both isomers and is due to the rotation of apical CO's. Simulation of the variable-temperature ^{13}C -NMR spectra using a 4×4 exchange matrix followed by *Eyring* regressions gave free enthalpies of activation of 50.2 ± 0.4 and 54.2 ± 0.5 kJ mol $^{-1}$ (at 298 K) for **12A** and **12R**, respectively. Once again, the higher ΔG^\ddagger of **12R** can be explained by the increased steric hindrance in the radial position on replacing a CO group by the bulky tertiary phosphine.

The general trends observed in the fluxional behaviour of derivatives of $[\text{Ir}_4(\text{CO})_{12}]$ and $[\text{Ir}_{4-x}\text{Rh}_x(\text{CO})_{12}]$ will be described in a forthcoming article of this series.

We thank the *Swiss National Science Foundation* for financial support, Dr. *Orrell* for a copy of the D2DNMR program, and Dr. *Suardi* for the characterisation of complexes **5** and **6**.

Experimental Part

1. *General*. See [1].

2. *Preparation of Complexes*. Clusters **2**, **3**, **7**, **10**, and **11** were prepared by the literature methods indicated in the text.

Nonacarbonyl(diamsine)(triphenylphosphine)tetrairidium ($[\text{Ir}_4(\text{CO})_9(\text{diars})\text{PPh}_3]$, **1**). A soln. of $[\text{Ir}_4(\text{CO})_{10}(\text{diars})]$ [24] (220 mg, 0.17 mmol), PPh_3 (44 mg, 0.17 mmol), and $\text{Me}_3\text{NO} \cdot 2 \text{H}_2\text{O}$ (19 mg, 0.17 mmol) in THF (100 ml) was stirred for 5 h at 0°. The suspension was filtered through a small column of silica gel and evaporated to dryness. The yellow residue was taken up in CH_2Cl_2 and chromatographed on a thick plate of silica gel using $\text{CH}_2\text{Cl}_2/\text{hexane}$ 1:3. The main fraction was extracted with CH_2Cl_2 and crystallised from $\text{CH}_2\text{Cl}_2/\text{MeOH}$ at -25° giving **1** (176 mg, 66%). IR (cyclohexane): 2029m, 2009m, 1982vs, 1967s, 1820s, 1773s (CO). ^{31}P -NMR: see text. ^{13}C -NMR (CD_2Cl_2 , 193 K): 229.7 (relative intensity 1.4, a_R); 223.3 (1, a_A); 213.5 (1, b_A); 209.1, 209.0 (2.4, b_R, b'_A); 207.1 (1.4, b'_R); 175.5 (d , 1.4, $J(\text{C},\text{P}) = 15$, d_R); 173.6 (d , 1, $J(\text{C},\text{P}) = 11$, f_A); 172.1 (1, d_A); 164.4, 161.0 (1 each, c_A, e'_A); 162.1, 159.5 (1.4 each, c_R, e'_R); 160.5 (d , 1, $^3J(\text{C},\text{P}) = 26$, g_A); 158.5 (1.4, h_R); 158.3, 158.2 (2.8, g_R, e_R); 155.1 (1, e_A). The signals of (c_A, e'_A) and of (c_R, e'_R) cannot be individually assigned but present a pseudo-*trans*-C, C-coupling in a 2D-COSY spectrum. Anal. calc. for $\text{As}_2\text{C}_{37}\text{H}_{31}\text{Ir}_4\text{O}_9\text{P}$ (1569.26): C 28.32, H 1.99; found: C 28.40, H 2.04.

Nonacarbonyl(methyldiphenylphosphine)(norbornadiene)tetrairidium ($[\text{Ir}_4(\text{CO})_9(\eta^4\text{-nbd})(\text{PMePh}_2)]$, **2**), and *Nonacarbonyl(norbornadiene)(triphenylphosphine)tetrairidium* ($[\text{Ir}_4(\text{CO})_9(\eta^4\text{-nbd})\text{PPh}_3]$, **3**). IR, ^1H -, and ^{31}P -NMR: see [17]. **2**: ^{13}C -NMR (CD_2Cl_2 , 193 K, signals grouped by isomer with $[\mathbf{2A}]/[\mathbf{2R}] = 1.8$): 217.3 (a_A); 208.4, 207.9 (b_A, b'_A); 174.2 (d , $J(\text{C},\text{P}) = 6$, f_A); 171.4 (d_A); 161.5, 158.6 (c_A, e'_A); 159.1 (d , $J(\text{C},\text{P}) = 28$, g_A); 154.2 (e_A); 218.1 (a_R); 209.1, 209.0 (b_R, b'_R); 173.3 (d , $J(\text{C},\text{P}) = 16$, d_R); 162.5, 153.9 (c_R, e'_R); 157.2 (g_R); 156.6 (e_R); 155.0 (d , $J(\text{C},\text{P}) \cong 4$, h_R). 2D-COSY (F2 = 3521 Hz): C, C couplings observed for signals of μ_2 -CO's and for the pairs (c_A, e'_A), (d_A, f_A), (c_R, e'_R), and (g_R, h_R).

Complex 3: ^{13}C -NMR ($\text{C}_2\text{D}_2\text{Cl}_4$, 240 K): 216.9 (1, b); 206.3 (2, a, b'); 172.8 (d , 1, $J(\text{C},\text{P}) = 5.7$, f); 169.6 (1, d); 160.6 (1, e'); 158.1 (d , 1, $J(\text{C},\text{P}) = 27.8$, g); 157.5 (1, c); 153.1 (1, e).

Nonacarbonyl[bis(diphenylphosphino)propane](methyldiphenylphosphine)tetrairidium ($[\text{Ir}_4(\text{CO})_9(\mu_2\text{-dppp})(\text{PMePh}_2)]$, **4**). A soln. of $[\text{Ir}_4(\text{CO})_{10}(\mu_2\text{-dppp})]$ (142 mg, 0.1 mmol) and PMePh_2 (21 μl , 0.11 mmol) in toluene (50 ml) was refluxed for 5 h, then evaporated to dryness. The orange residue was taken up in CH_2Cl_2 and chromatographed on a thick plate of silica gel using $\text{CH}_2\text{Cl}_2/\text{hexane}$ 1:1. Extraction of a first yellow fraction with CH_2Cl_2 and crystallisation from $\text{CH}_2\text{Cl}_2/\text{hexane}$ at -25° gave **4** (35 mg, 23%). The second yellow fraction gave $[\text{Ir}_4(\text{CO})_8(\mu_2\text{-dppp})(\text{PMePh}_2)_2]$. IR (cyclohexane): 2046s, 2038s, 2001s, 1994s, 1799m, 1785m (CO). ^{31}P -NMR (CD_2Cl_2 , r.t.): -8.6 ($\Delta\delta = 19.5$ with respect to free PMePh_2); -17.2 ($\Delta\delta = 0.1$ with respect to free dppp). ^{13}C -NMR (CD_2Cl_2 , 290 K): 218.3 (1, a); 213.4 (2, b); 176.3 (dd , 2, $J(\text{C},\text{P}) = 6$, 16, f); 164.4 (d , 1, $J(\text{C},\text{P}) = 7.9$, c); 160.8 (d , 2, $J(\text{C},\text{P}) = 27.7$, g); 157.7 (1, e). Anal. calc. for $\text{C}_{49}\text{H}_{39}\text{Ir}_4\text{O}_9\text{P}_3$ (1633.65): C 36.03, H 2.41; found: C 36.50, H 2.47.

Nonacarbonyl[tris(methylthio)]methanetetrairidium ($[\text{Ir}_4(\text{CO})_9\{\mu_3\text{-HC}(\text{SCH}_3)_3\}]$, **5**). A soln. of $[\text{Ir}_4(\text{CO})_{11}]^-$ (450 mg, 0.337 mmol), $\text{HC}(\text{SCH}_3)_3$ (54 mg, 0.35 mmol), and AgBF_4 (65.6 mg, 0.337 mmol) in THF (150 ml) was stirred at -20° for 1 h. After filtration of AgI, the soln. was heated at 50° for 4 h, then evaporated to a small volume.

Chromatography on a thick plate of silica gel using CH_2Cl_2 /hexane 2:3 and extraction of the first yellow fraction gave **5** (230 mg, 58%) after crystallisation from CH_2Cl_2 /hexane at -25° . The second yellow fraction gave $[\text{Ir}_4(\text{CO})_{10}\{\mu_2\text{-HC}(\text{SCH}_3)_3\}]$ (12%). IR (cyclohexane): 2081*m*, 2043*s*, 2021*s*, 1983 (sh), 1967 (sh) (CO). $^{13}\text{C-NMR}$ (CD_2Cl_2 , 190 K): 166.2, 166.1 (1 each, *a, b*); 156.4 (1, *e*). Anal. calc. for $\text{C}_{13}\text{H}_{10}\text{Ir}_4\text{O}_9\text{S}_3$ (1175.28): C 13.29, H 0.86; found: C 13.12, H 0.92.

Nonacarbonyl $\{1,3\text{-bis}(\text{diphenylphosphino})\text{-}2\text{-}[(\text{diphenylphosphino})\text{methyl}]\text{-}2\text{-methylpropane}\}$ *tetrairidium* ($[\text{Ir}_4(\text{CO})_9\{\mu_3\text{-H}_3\text{CC}(\text{CH}_2\text{PPh}_2)_3\}]$, **6**). A soln. of $[\text{Ir}_4(\text{CO})_{11}]^-$ (300 mg, 0.224 mmol), triphos (156.2 mg, 0.250 mmol), and AgBF_4 (46.7 mg, 0.24 mmol) in THF (100 ml) was stirred at r.t. for 1 h, filtered, and refluxed for 3 h. Evaporation to dryness and chromatography of the yellow residue on a thick plate of silica gel using CH_2Cl_2 /hexane 1:1 gave **6** (256 mg, 69%) after crystallisation from CH_2Cl_2 /hexane at -25° . IR (THF): 2044*s*, 1991*s*, 1792*s* (CO). $^{13}\text{C-NMR}$ (CD_2Cl_2 , 203 K): 217.6 (1, *a*); 177.5 (1, *d*); 158.9 (*d*, $^3J(\text{C,P}) = 30$, *g*). Anal. calc. for $\text{C}_{49}\text{H}_{39}\text{Ir}_4\text{O}_9\text{P}_3$ (1633.65): C 36.03, H 2.41, P 5.69; found: C 36.87, H 2.53, P 5.65.

Octacarbonylbis(cycloocta-1,5-diene)tetrairidium ($[\text{Ir}_4(\text{CO})_8(\eta^4\text{-cod})_2]$, **7**), *Octacarbonyl(cycloocta-1,5-diene)-(norbornadiene)tetrairidium* ($[\text{Ir}_4(\text{CO})_8(\eta^4\text{-cod})(\eta^4\text{-nbd})]$, **8**), and *Octacarbonylbis(norbornadiene)tetrairidium* ($[\text{Ir}_4(\text{CO})_8(\eta^4\text{-nbd})_2]$, **9**). An example of synthesis is given for **8**. A soln. of $[\text{Ir}_4(\text{CO})_{10}(\eta^4\text{-cod})]$ (93 mg, 0.08 mmol), nbd (109 μl , 1 mmol), and $\text{Me}_3\text{NO}\cdot 2\text{H}_2\text{O}$ (17 mg, 1.6 mmol) in THF (40 ml) was stirred for 6 h at -10° , while following the disappearance of the starting complex by TLC (CH_2Cl_2 /hexane 1:2). The soln. was evaporated at r.t. to 5 ml, dried (CaSO_4), and chromatographed on a column (Lobar B, Lichroprep Si 60, 40–63 μm) using CH_2Cl_2 /hexane 1:4. Crystallisation from CH_2Cl_2 /hexane at -25° gave **8** as orange microcrystals (60 mg, 63%).

Complex 7: see [14]. $^{13}\text{C-NMR}$ (CD_2Cl_2 , 290 K): 220.2 (1, *a*); 212.1 (2, *b*); 176.3 (1, *d*); 162.1, 154.4 (1 each, *e, c*); 156.6 (2, *g*). 2D-EXSY (CD_2Cl_2 , 290 K, mixing time 100 ms): cross-peaks observed between signals at 162.1 and 156.6 ppm only. Variable-temperature $^{13}\text{C-NMR}$ spectra simulated from 270 to 330 K ($k_1 = 5 \pm 1$ and $72 \pm 29 \text{ s}^{-1}$, respectively).

Complex 8: IR (CH_2Cl_2): 2091*m*, 2056*s*, 2032 (sh), 2001*s*, 1989 (br.), 1809*s*, 1791*s* (CO). $^1\text{H-NMR}$ (CD_2Cl_2 , 298 K): 4.65, 4.50, 4.22 (3*m*, 4, H–C(2,3,5,6) of nbd); 4.00, 3.90 (2*m*, 2, H–C(1,4) of nbd); 1.05 (*m*, 2, H–C(7) of nbd); 4.65, 4.43 (2*m*, 4, cod); 4.38, 3.38, 3.10, 2.75, 2.35, 2.10, 1.65, 1.50 (8*m*, 8, cod). $^{13}\text{C-NMR}$ (CD_2Cl_2 , 220 K): 219.8 (1, *a*); 212.8, 209.9 (1 each, *b, b'*); 174.6 (1, *d*); 162.1 (1, *e*); 156.7, 155.8 (1 each, *g, g'*); 153.8 (1, *c*). Variable-temperature $^{13}\text{C-NMR}$ spectra simulated from 220 to 290 K ($k_1 = 15 \pm 4$ and $1751 \pm 310 \text{ s}^{-1}$, resp.) using the matrix elements (e, e) = (g, g) = (g', g') = $-k_1$, (g', e) = (e, g) = (g, g') = k_1 . Anal. calc. for $\text{C}_{23}\text{H}_{20}\text{Ir}_4\text{O}_8$ (1193.2): C 23.15, H 1.69; found: C 22.94, H 1.59.

Complex 9: IR (cyclohexane): 2083*m*, 2055*s*, 2021*s*, 2007*m*, 1836*s*, 1821*s* (CO). $^1\text{H-NMR}$ (CD_2Cl_2 , 173 K): 4.55, 4.43, 3.88 (3*m*, 2 each); 1.11 (*m*, 2, H–C(7)). $^{13}\text{C-NMR}$ (CD_2Cl_2 , 173 K): 207.5 (2, *a*); 198.2 (1, *b*); 170.4 (2, *d*); 158.6 (2, *e*); 151.7 (2, *g*); 151.4 (2, *c*). 2D-EXSY (213 K, mixing time 100 ms): cross-peaks observed between signals at 158.6 and 151.7 ppm only. Variable-temperature $^{13}\text{C-NMR}$ spectra simulated from 213 to 283 K ($k_1 = 78 \pm 10$ and $14918 \pm 1670 \text{ s}^{-1}$, respectively).

Octacarbonylbis[1,3-bis(diphenylphosphino)propane]tetrairidium ($[\text{Ir}_4(\text{CO})_8(\mu_2\text{-dppp})_2]$, **10**) and *Octacarbonylbis[bis(diphenylphosphino)methane]tetrairidium* ($[\text{Ir}_4(\text{CO})_8(\mu_2\text{-dppm})_2]$, **11**). *Complex 10*. A suspension of $[\text{Ir}_4(\text{CO})_{12}]$ (276 mg, 0.25 mmol) and dppp (220 mg, 0.53 mmol) in THF (150 ml) was refluxed for 16 h, and the resulting orange soln. evaporated to dryness. The residue was taken up in CH_2Cl_2 and chromatographed on a thick plate of silica gel using hexane/ CH_2Cl_2 3:2. A first fraction contained $[\text{Ir}_4(\text{CO})_{10}(\mu_2\text{-dppp})]$. Extraction of the second fraction with CH_2Cl_2 and crystallisation from hexane/ CH_2Cl_2 at -25° gave **11** (282 mg, 63%) as orange crystals. IR (THF): 2005*s*, 1980*vs*, 1945*s*, 1840*w*, 1780*s*, 1760*s* (CO). $^{31}\text{P-NMR}$ (CD_2Cl_2 , r.t.): -1.7 (1, P_3); -29.2 (*d*, $J(\text{P,P}) = 90.3$, P_1); -29.2 (1, P_2); -48.0 (*d*, P_4). Small couplings were observed at 32.2 MHz (*Varian FT-80A*): $J(\text{P}_1, \text{P}_2) = \pm 5.3$; $J(\text{P}_1, \text{P}_3) = \pm 2.0$; $J(\text{P}_2, \text{P}_3) = \pm 3.1$; $J(\text{P}_2, \text{P}_4) = \pm 1.7$; $J(\text{P}_3, \text{P}_4) = \pm 2.5$. $^{13}\text{C-NMR}$ (CD_2Cl_2 , 290 K): 226.0 (*d*, $J(\text{C,P}) = 8$), 219.5 (*d*, $J(\text{C,P}) = 3$), 208.7 (*s*, 1 each, *b, a, b'*); 178.0; 177.7 (2*dd*, 1 each, $J(\text{C,P}) = 17$, 8, *f, f'*); 172.0 (*d*, $J(\text{C,P}) = 32$, *g*); 168.4 (*d*, $J(\text{C,P}) = 4.6$, *e*); 165.3 (*d*, $J(\text{C,P}) = 7.6$, *c*). Anal. calc. for $\text{C}_{62}\text{H}_{52}\text{Ir}_4\text{O}_8\text{P}_4$ (1817.87): C 40.96, H 2.88; found: C 41.08, H 3.10.

Complex 11; see [21]. $^{31}\text{P-NMR}$ (CD_2Cl_2 , 190 K): -24.5 (*d*, $J(\text{P,P}) = 44$, P_3); -45.9 (*dd*, $J(\text{P,P}) = 102$, 44, P_1); -50.7 (*d*, P_1); -62.4 (*dd*, P_4). $^{13}\text{C-NMR}$ (CD_2Cl_2 , 185 K): 222.4, 217.5, 214.3 (1 each, *b, a, b'*); 183.2, 182.2 (1 each, *f', f*); 172.9, 170.9 (1 each, *e, c*); 166.4 (*d*, $J(\text{C,P}) = 36.8$, *g*).

3. 2D-EXSY Spectra. The $^{31}\text{P-NMR}$ spectra of **10** and **11** were recorded on a Bruker AC-200 (81.01 MHz) in CD_2Cl_2 or $\text{C}_2\text{D}_2\text{Cl}_4$ in a sealed 5-mm tube, and their $^{13}\text{C-NMR}$ spectra on a Bruker WH-360 (90.55 MHz) in a sealed 10-mm tube, without decoupling using the TPPI method [25]. No random variation of t_m was used since ^{13}C -scalar couplings were not observed. For the quantitative analysis, t_1 increments of 2-K transients were recorded with a spectral width of 6757 Hz (F2) (6886 Hz for ^{31}P). The mixing times are indicated in the text. Before

Fourier transformation, a square cosine bell was applied in both domains and the FID's were zero filled to 2-K in the F1 domain. Peak integrals were obtained using the *Bruker* routine in DISNMR. Errors in the peak integrals were estimated by measuring integrals using the same area as for the peak but offset in the F1 and F2 directions, as close to the peak as was possible, giving values ϵ_1 and ϵ_2 , resp. The standard error σ in the peak integral was then taken as $\sigma = \sqrt{(\epsilon_1^2 + \epsilon_2^2)}$. The values entered into the program D2DNMR were the averages of symmetrically equivalent cross-peaks, the integrals of the diagonal peaks, and the corresponding σ 's. Where no peak was observed, the integral was taken as zero and the σ as the smallest σ value found for the observed peaks.

REFERENCES

- [1] A. Strawczynski, G. Suardi, R. Ros, R. Roulet, F. Grepioni, D. Braga, *Helv. Chim. Acta* **1993**, *76*, 2210.
- [2] B. E. Mann, C. M. Spencer, A. K. Smith, *J. Organomet. Chem.* **1983**, *244*, C17.
- [3] B. E. Mann, B. T. Pickup, A. K. Smith, *J. Chem. Soc., Dalton Trans.* **1989**, 889.
- [4] G. F. Stuntz, J. R. Shapley, *J. Am. Chem. Soc.* **1977**, *99*, 607.
- [5] B. E. Mann, M. D. Vargas, R. Khadar, *J. Chem. Soc., Dalton Trans.* **1992**, 1725.
- [6] K. Besançon, G. Laurency, T. Lumini, R. Roulet, G. Gervasio, *Helv. Chim. Acta* **1993**, *76*, 2926.
- [7] M. Davis, R. Roulet, *Inorg. Chim. Acta* **1992**, *197*, 15.
- [8] A. Strawczynski, R. Ros, R. Roulet, *Helv. Chim. Acta* **1988**, *71*, 867.
- [9] D. Braga, R. Ros, R. Roulet, *J. Organomet. Chem.* **1985**, *286*, C8.
- [10] G. F. Stuntz, J. R. Shapley, *J. Organomet. Chem.* **1981**, *213*, 389.
- [11] A. Orlandi, R. Ros, R. Roulet, *Helv. Chim. Acta* **1991**, *74*, 1464.
- [12] G. Bondietti, R. Ros, R. Roulet, F. Musso, G. Gervasio, *Inorg. Chim. Acta* **1993**, *213*, 301.
- [13] A. Strawczynski, R. Ros, R. Roulet, F. Grepioni, D. Braga, *Helv. Chim. Acta* **1988**, *71*, 1885.
- [14] G. F. Stuntz, J. R. Shapley, C. G. Pierpont, *Inorg. Chem.* **1978**, *17*, 2596.
- [15] G. Suardi, A. Strawczynski, R. Ros, R. Roulet, F. Grepioni, D. Braga, *Helv. Chim. Acta* **1990**, *73*, 154.
- [16] A. Orlandi, U. Frey, G. Suardi, A. E. Merbach, R. Roulet, *Inorg. Chem.* **1992**, *31*, 1304.
- [17] D. Braga, F. Grepioni, G. Guadalupi, A. Scrivanti, R. Ros, R. Roulet, *Organometallics* **1987**, *6*, 56.
- [18] J. A. Lucas, M. M. Harding, B. S. Nicholls, A. K. Smith, *J. Chem. Soc., Chem. Commun.* **1984**, 319.
- [19] R. Ros, A. Scrivanti, R. Roulet, *J. Organomet. Chem.* **1986**, *303*, 273.
- [20] G. Bondietti, Thèse de doctorat n° 1135, EPF-Lausanne, 1993; G. Bondietti, G. Suardi, R. Ros, R. Roulet, F. Grepioni, D. Braga, *Helv. Chim. Acta* **1993**, *76*, 2913.
- [21] M. M. Harding, B. S. Nicholls, A. K. Smith, *Acta Crystallogr., Sect. C* **1984**, *40*, 790.
- [22] E. W. Abel, T. P. J. Coston, K. G. Orrell, V. Sik, S. Stephenson, *J. Magn. Reson.* **1986**, *70*, 34.
- [23] E. W. Abel, I. Moss, K. G. Orrell, V. Sik, D. Stephenson, *J. Chem. Soc., Dalton Trans.* **1987**, 2695; L. J. Farrugia, Y. Chi, W.-C. Tu, *Organometallics* **1993**, *12*, 1616.
- [24] J. R. Shapley, G. F. Stuntz, M. R. Churchill, J. P. Hutchinson, *J. Am. Chem. Soc.* **1979**, *101*, 7425.
- [25] G. Bodenhausen, H. Kogler, R. R. Ernst, *J. Magn. Reson.* **1984**, *58*, 370.